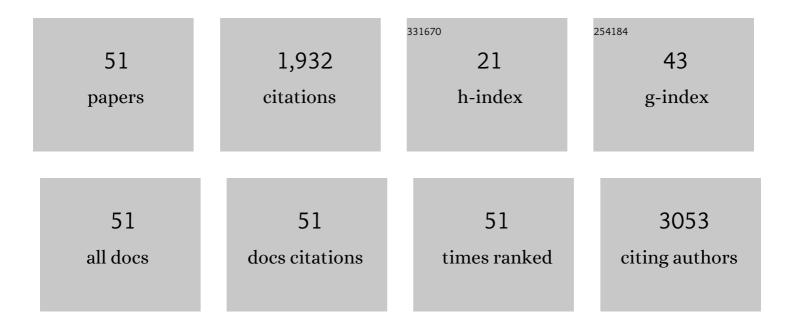
S Aminorroaya Yamini

List of Publications by Year in descending order

Source: https://exaly.com/author-pdf/3502794/publications.pdf Version: 2024-02-01



#	Article	IF	CITATIONS
1	Scalable Oneâ€6tep Wetâ€6pinning of Graphene Fibers and Yarns from Liquid Crystalline Dispersions of Graphene Oxide: Towards Multifunctional Textiles. Advanced Functional Materials, 2013, 23, 5345-5354.	14.9	354
2	High-Performance Multifunctional Graphene Yarns: Toward Wearable All-Carbon Energy Storage Textiles. ACS Nano, 2014, 8, 2456-2466.	14.6	331
3	Magnetism-mediated thermoelectric performance of the Cr-doped bismuth telluride tetradymite. Materials Today Physics, 2019, 9, 100090.	6.0	112
4	Enhanced Hydrogen Storage in Graphene Oxideâ€MWCNTs Composite at Room Temperature. Advanced Energy Materials, 2012, 2, 1439-1446.	19.5	97
5	Recent progress in magnesium-based thermoelectric materials. Journal of Materials Chemistry A, 2018, 6, 3328-3341.	10.3	70
6	Globular reduced graphene oxide-metal oxide structures for energy storage applications. Energy and Environmental Science, 2012, 5, 5236-5240.	30.8	69
7	Thermoelectric Performance of <i>n</i> -Type (PbTe) _{0.75} (PbS) _{0.15} (PbSe) _{0.1} Composites. ACS Applied Materials & Interfaces, 2014, 6, 11476-11483.	8.0	69
8	Heterogeneous Distribution of Sodium for High Thermoelectric Performance of pâ€ŧype Multiphase Leadâ€Chalcogenides. Advanced Energy Materials, 2015, 5, 1501047.	19.5	63
9	The effect of transition metals on hydrogen migration and catalysis in cast Mg–Ni alloys. International Journal of Hydrogen Energy, 2011, 36, 4984-4992.	7.1	60
10	Hydrogen storage properties of Mg-10Âwt% Ni alloy co-catalysed with niobium and multi-walled carbon nanotubes. International Journal of Hydrogen Energy, 2011, 36, 571-579.	7.1	56
11	Rational design of p-type thermoelectric PbTe: temperature dependent sodium solubility. Journal of Materials Chemistry A, 2013, 1, 8725.	10.3	56
12	Chemical composition tuning in quaternary p-type Pb-chalcogenides – a promising strategy for enhanced thermoelectric performance. Physical Chemistry Chemical Physics, 2014, 16, 1835-1840.	2.8	48
13	Processable 2D materials beyond graphene: MoS ₂ liquid crystals and fibres. Nanoscale, 2016, 8, 16862-16867.	5.6	40
14	Microstructure and activation characteristics of Mg–Ni alloy modified by multi-walled carbon nanotubes. International Journal of Hydrogen Energy, 2010, 35, 4144-4153.	7.1	39
15	Alendronate improves fasting plasma glucose and insulin sensitivity, and decreases insulin resistance in prediabetic osteopenic postmenopausal women: A randomized tripleâ€blind clinical trial. Journal of Diabetes Investigation, 2019, 10, 731-737.	2.4	37
16	Thermoelectric Performance of Na-Doped GeSe. ACS Omega, 2017, 2, 9192-9198.	3.5	34
17	One-step bonding of Ni electrode to n-type PbTe $\hat{a} \in$ " A step towards fabrication of thermoelectric generators. Materials and Design, 2016, 107, 90-97.	7.0	33
18	Thermoelectric performance of tellurium-reduced quaternary p-type lead–chalcogenide composites. Acta Materialia, 2014, 80, 365-372.	7.9	28

#	Article	IF	CITATIONS
19	Band-Gap Nonlinearity in Lead Chalcogenide (PbQ, Q = Te, Se, S) Alloys. ACS Omega, 2017, 2, 3417-3423.	3.5	28
20	Fabrication and characterization of textured Bi2Te3 thermoelectric thin films prepared on glass substrates at room temperature using pulsed laser deposition. Journal of Crystal Growth, 2013, 362, 247-251.	1.5	24
21	Diabetes and all-cause mortality, a 18-year follow-up study. Scientific Reports, 2020, 10, 3183.	3.3	24
22	Recent Progress in Multiphase Thermoelectric Materials. Materials, 2021, 14, 6059.	2.9	23
23	Thermoelectric performance of n-type Mg2Ge. Scientific Reports, 2017, 7, 3988.	3.3	21
24	Body mass index and the all-cause mortality rate in patients with type 2 diabetes mellitus. Acta Diabetologica, 2018, 55, 569-577.	2.5	19
25	Thermoelectric Performance of n-Type Magnetic Element Doped Bi ₂ S ₃ . ACS Applied Energy Materials, 2022, 5, 3845-3853.	5.1	19
26	Fabrication of thermoelectric materials – thermal stability and repeatability of achieved efficiencies. Journal of Materials Chemistry C, 2015, 3, 10610-10615.	5.5	17
27	Elemental distributions within multiphase quaternary Pb chalcogenide thermoelectric materials determined through three-dimensional atom probe tomography. Nano Energy, 2016, 26, 157-163.	16.0	15
28	Solid-State Bonding of Bulk PbTe to Nickel Electrode for Thermoelectric Modules. ACS Applied Energy Materials, 2018, 1, 348-354.	5.1	14
29	Thyroidâ€stimulating hormone (TSH) serum levels and risk of spontaneous abortion: A prospective populationâ€based cohort study. Clinical Endocrinology, 2019, 91, 163-169.	2.4	14
30	Rapid fabrication of diffusion barrier between metal electrode and thermoelectric materials using current-controlled spark plasma sintering technique. Journal of Materials Research and Technology, 2019, 8, 8-13.	5.8	12
31	Comparison of hydrogen storage properties of Mg–Ni from different preparation methods. Materials Chemistry and Physics, 2011, 127, 405-408.	4.0	11
32	Thermoelectric performance of thermally aged nanostructured bulk materials—a case study of lead chalcogenides. Materials Today Physics, 2020, 13, 100190.	6.0	11
33	Crystal structure, electronic structure and thermoelectric properties of n-type BiSbSTe2. Journal Physics D: Applied Physics, 2012, 45, 125301.	2.8	9
34	Origin of resistivity anomaly in p-type leads chalcogenide multiphase compounds. AIP Advances, 2015, 5, 053601.	1.3	9
35	Reference Intervals for Thyroid Hormones During the First Trimester of Gestation: A Report from an Area with a Sufficient Iodine Level. Hormone and Metabolic Research, 2019, 51, 165-171.	1.5	8
36	Effect of the Fabrication Technique on the Thermoelectric Performance of Mg-Based Compounds—A Case Study of n-Type Mg ₂ Ge. ACS Omega, 2017, 2, 8069-8074.	3.5	7

#	Article	IF	CITATIONS
37	Thermoelectric Performance of Single Phase p-Type Quaternary (PbTe) _{0.65–<i>x</i>} (PbSe) _{0.35} (PbS) _{<i>x</i>} Alloys. ACS Applied Energy Materials, 2018, 1, 1898-1903.	5.1	7
38	TEM characterization of precipitates in the segregated regions of a lowâ€carbon, lowâ€manganese, titaniumâ€added steel. Journal of Microscopy, 2007, 227, 92-97.	1.8	6
39	A novel approach to simulate segregation at the centreline of continuously cast steel using laser-scanning confocal microscopy. Journal of Microscopy, 2007, 227, 87-91.	1.8	5
40	TEM analysis of centreline sulphide precipitates modified by titanium additions to low carbon steel. Journal of Microscopy, 2008, 232, 123-129.	1.8	5
41	<p>Cross-sectional and longitudinal assessments of risk factors associated with hypertension and moderately increased albuminuria comorbidity in patients with type 2 diabetes: a 9-year open cohort study</p> . Diabetes, Metabolic Syndrome and Obesity: Targets and Therapy, 2019, Volume 12. 1123-1139.	2.4	4
42	Multiphase identification in Ni–PbTe contacts by EBSD and aberration-corrected STEM. Materials and Design, 2020, 185, 108252.	7.0	4
43	Simulation of microsegregation and the solid/liquid interface progression in the concentric solidification technique. Modelling and Simulation in Materials Science and Engineering, 2011, 19, 025003.	2.0	3
44	Assessing phase discrimination <i>via</i> the segmentation of an elemental energy dispersive X-ray spectroscopy map: a case study of Bi ₂ Te ₃ and Bi ₂ Te _{S. RSC Advances, 2018, 8, 7457-7464.}	3.6	3
45	Suspension Characteristics and Electrophoretic Deposition ofp-Type Bi2Te3Films for Thermoelectric Applications. Journal of the Electrochemical Society, 2018, 165, D364-D369.	2.9	3
46	Mechanically induced combustion synthesis and thermoelectric properties of nanostructured strontium hexaboride (SrB6). Ceramics International, 2019, 45, 14426-14431.	4.8	3
47	In situ characterisation of nanostructured multiphase thermoelectric materials at elevated temperatures. Physical Chemistry Chemical Physics, 2016, 18, 32814-32819.	2.8	2
48	Thermoelectric Performance of Single-Phase Tellurium-Reduced Quaternary (PbTe) _{0.55} (PbS) _{0.1} (PbSe) _{0.35} . ACS Omega, 2019, 4, 9235-9240.	3.5	2
49	Influence of microalloying elements (Ti, Nb) and nitrogen concentrations on precipitation of pipeline steels—A thermodynamic approach. Engineering Reports, 2021, 3, e12337.	1.7	2
50	Thermoelectric Properties and Microstructure Studies of Spinodally Decomposed PbTe _{0.38} S _{0.62} Alloy. Science of Advanced Materials, 2014, 6, 1453-1459.	0.7	2
51	Hydrogen Storage Properties of Mg-Ni Alloy Catalysed by Multi-Walled Carbon Nanotubes. Materials Science Forum, 2010, 654-656, 2843-2846.	0.3	0